Int. J. Heat Mass Transfer. Vol. 16, pp. 1215-1229. Pergamon Press 1973. Printed in Great Britain

THEORETICAL INVESTIGATION ON LAMINAR BOUNDARY LAYER WITH COMBUSTION ON A FLAT PLATE

SHINZO KIKKAWA and KATSUHIRO YOSHIKAWA

Department of Mechanical Engineering, Doshisha University, Kamikyo-ku, Kyoto, Japan

(*Received* 6 *May* 1972)

Abstract—The problems of the laminar boundary layer where combustion reaction occurs are solved theoretically taking account of the Arrhenius' theory of chemical kinetics, of the effects of the impermeable leading section, and of the fact that the properties of fluid depend on the temperature and concentrations of species contained in the boundary layer. As the result of this investigation, the following conclusions have been obtained:

(1) The maximum temperature obtained in the present work is lower by about several hundred degrees of centigrade than that by the method which has been used in the previously published papers,

(2) The combustion zone occupies about 20 per cent of the boundary layer in width,

(3) In the case of using the test plate with an impermeable leading section, the boundary layer thickness increases and the maximum temperature goes down compared with the case using the test plate without impermeable leading section. The impermeable leading section has a great influence on the shear stress at the wall,

(4) In the case of uniformly injecting the gaseous fuel from the wall, the fuel concentration at the wall and the maximum temperature change with the distance from the leading edge.

NOMENCLATURE

c_p, specific heat at constant pressure;
D, multicomponent diffusion coefficient;
$\mathscr{D}$, binary diffusion coefficient;
E_A, activation energy;
g, acceleration of gravity;
h, enthalpy;
L, latent heat of vaporization;
Le, Lewis number;
l, length of impermeable leading section;
M, molecular weight;
Pr, Prandtl number;
Q, calorific value of fuel;
q, heat flux;
R, universal gas constant;
Sc, Schmidt number;
T, absolute temperature;
t, temperature in degree of centigrade;
u, velocity in x-direction;
v, velocity in y-direction;
W, mass fraction of species;
x, coordinate parallel to plate;
y, coordinate perpendicular to plate;
Z, mass rate of formation of fuel.

Greek

β, mass transfer ratio;
η, transformed coordinate (see equation (15));
λ, thermal conductivity;
μ, coefficient of dynamic viscosity;
ξ, transformed coordinate (see equation (14));
π, stoichiometric constant;
ρ, density;
χ, frequency factor.

Subscripts

e, free stream flow;
i, j, species i, j;
r, reference condition;
t, fuel reservoir;
w, upper surface of test plate;
δ, outer edge of boundary layer;

0, leading edge.
Quantities without subscript i or j denote those of mixed gas.

Superscript
*, with impermeable leading section.

1. INTRODUCTION

MANY theoretical investigations on the diffusion flame have been published. Most of them in the early years have treated the combustion of a droplet as a spherically symmetric phenomenon based on the assumptions that the rate of chemical reaction is infinite, the properties of fluid are constant, and heat and mass are transferred only by conduction and diffusion, not by convection [1–4]. With development of the jet and rocket engines, the burning process in the boundary layer on a flat plate have been solved taking account of the convective heat and mass transfer [5–7].

These papers, however, simplify the problem by assuming that the rate of chemical reaction is infinite, the properties of fluid are independent of temperature and concentration of species, and the profiles of velocity, temperature and concentrations have linear relation with each other.

The first attempt introducing Arrhenius' theory of chemical kinetics into the theory of combustion process was performed by J. Lorell *et al.* [8] but the same assumptions used in literatures [1–4] were applied in this study except the Arrhenius' theory. F. E. Fendell [9] and Y. Mori *et al.* [10] have got the very interesting results for the counter flow diffusion flame taking account of Arrhenius' theory. However, these studies basing on Euler's equation but not on Navier–Stokes' equation assume that every property is constant, Prandtl number and Lewis number are unity, and the temperature at the wall is equal to the boiling point of fuel.

The above papers [8, 9] point out that the temperature profile in combustion zone, particularly the maximum temperature is strongly affected by introducing the finite rate of chemical reaction. As it is apparent that the properties of fluid have a great effect on the burning condition, the assumption that the properties are kept constant across the boundary layer is different from the actual condition in a great deal, because the temperature and the concentrations of species across the boundary layer change remarkably.

There have never been published the papers taking account of all the above factors and the effect of impermeable leading section. In this paper, the diffusion flame in the laminar boundary layer is dealt with taking account of these factors, but the effects of free convection and thermal dissociation are neglected. For comparison, the calculations for the flame sheet model are performed.

2. GOVERNING EQUATIONS AND BOUNDARY CONDITIONS

Considering the combustion of hydrocarbon fuel, the chemical reaction is given as follows

$$\pi_1\,(\text{fuel vapor}) + \pi_2 O_2 + \pi_3 CO_2 + \pi_4 H_2O = 0. \qquad (1)$$

In the case using methyl alcohol as a fuel, the stoichiometric constants are

$$\pi_1 = 1, \quad \pi_2 = 3/2, \quad \pi_3 = -1, \quad \pi_4 = -2.$$

Taking air as the oxidizer and considering that air is a mixed gas of oxygen and nitrogen only, the species contained in the boundary layer are as follows; (1) fuel vapor, (2) oxygen, (3) carbon dioxide, (4) water vapor and (5) nitrogen because of neglecting thermal dissociation. Henceforward, the subscripts 1–5 denote the above species respectively.

The mass rate of formation of fuel Z is of a value of negative sign, and according to the Arrhenius' theory of chemical kinetics, it is shown as

$$Z = -(\chi \rho g W_1 W_2 M/M_2) \exp(-E_A/RT). \qquad (2)$$

Considering the model shown in Fig. 1, the following governing equations are obtained.
Equation of continuity,

$$\frac{\partial}{\partial x}(\rho u) + \frac{\partial}{\partial y}(\rho v) = 0 \tag{3}$$

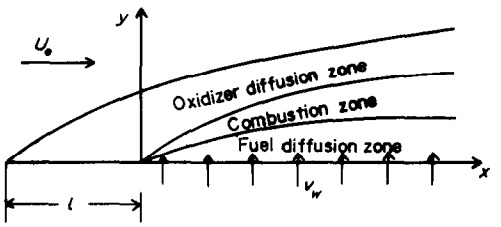

FIG. 1. Diffusion flame model.

Equation of momentum,

$$\rho\left(u\frac{\partial u}{\partial x} + v\frac{\partial u}{\partial y}\right) = \frac{\partial}{\partial y}\left(\mu\frac{\partial u}{\partial y}\right) \tag{4}$$

Equation of energy,

$$\rho\left(u\frac{\partial h}{\partial x} + v\frac{\partial h}{\partial y}\right) = \frac{\partial}{\partial y}\left[\frac{\lambda}{gC_p}\frac{\partial h}{\partial y} + \sum_{i=1}^{5}\left\{\rho D_i h_i(1 - Le_i)\frac{\partial W_i}{\partial y}\right\}\right] - \frac{QZ}{g} \tag{5}$$

Equations of continuity of species,

$$\rho\left(u\frac{\partial W_i}{\partial x} + v\frac{\partial W_i}{\partial y}\right) = \frac{\partial}{\partial y}\left(\rho D_i\frac{\partial W_i}{\partial y}\right) + \frac{\pi_i M_i Z}{g} \qquad i = 1\text{–}4, \tag{6}\text{–}(9)$$

$$\sum_{i=1}^{5} W_i = 1. \tag{10}$$

As shown in the above equations (2)–(10), nine unknown quantities u, v, h, w_1–w_5 and Z are contained, these unknown quantities might be solved as functions of x and y on the several boundary conditions.

Introducing the following new variables into the above equations,

$$f' = u/u_e \tag{11}$$

$$\theta = (h - h_w)/\Delta h \qquad \Delta h = h_e - h_w \tag{12}$$

$$\zeta_i = (W_i - W_w)/W_{ir} \qquad i = 1\text{–}5 \tag{13}$$

and transforming x–y coordinates into $\xi - \eta$ coordinates defined as follows, we get the equations (16)–(23).

$$\xi = u_e\int_0^x (\rho\mu)_r\,dx \tag{14}$$

$$\eta = \frac{u_e}{\sqrt{(2\xi)}}\int_0^y \rho\,dy \tag{15}$$

Equation of continuity,

$$2\xi\frac{\partial f'}{\partial \xi} + \frac{\partial V}{\partial \eta} + f' = 0 \tag{16}$$

Equation of momentum,

$$2\xi f'\frac{\partial f'}{\partial \xi} + V\frac{\partial f'}{\partial \eta} = \frac{\partial}{\partial \eta}\left(A\frac{\partial f'}{\partial \eta}\right) \qquad A = \frac{\rho\mu}{(\rho\mu)_r} \tag{17}$$

Equation of energy,

$$2\xi f'\frac{\partial \theta}{\partial \xi} + V\frac{\partial \theta}{\partial \eta} = \frac{\partial}{\partial \eta}\left(B\frac{\partial \theta}{\partial \eta} + \sum_{i=1}^{5} C_i\frac{\partial \zeta_i}{\partial \eta}\right) + D$$

$$B = \frac{\rho\mu}{(\rho\mu)_r}\frac{1}{P_r}, \qquad C_i = \frac{\rho^2 D_i h_i W_{ir}(1 - Le_i)}{\Delta h(\rho\mu)_r}, \qquad D = \frac{-2\xi QZ}{u_e^2(\rho\mu)_r\Delta h\rho g} \tag{18}$$

Equations of continuity of species,

$$2\xi f'\frac{\partial \zeta_i}{\partial \xi} + V\frac{\partial \zeta_i}{\partial \eta} = \frac{\partial}{\partial \eta}\left(E_i\frac{\partial \zeta_i}{\partial \eta}\right) + F_i \qquad i = 1\text{–}4 \tag{19}\text{–}(22)$$

$$E_i = \frac{\rho\mu}{(\rho\mu)_r}\frac{1}{Sc_i}, \qquad F_i = \frac{2\xi Z M_i\pi_i}{u_e^2(\rho\mu)_r g W_{ir}\rho}$$

$$\sum_{i=1}^{5}\zeta_i W_{ir} = 0 \tag{23}$$

where,

$$V = \frac{2\xi}{(\rho\mu)_r u_e}\left(f'\frac{\partial\eta}{\partial x} + \frac{\rho v}{\sqrt{(2\xi)}}\right). \quad (24)$$

The boundary conditions at the wall are as follows,

$$f'(\xi, 0) = 0 \quad (25)$$

$$\theta(\xi, 0) = 0 \quad (26)$$

$$\zeta_i(\xi, 0) = 0 \qquad i = 1\text{–}5 \quad (27)\text{–}(31)$$

$$V(\xi, 0) = \sqrt{(2\xi)}\,(\rho v)_w/\{(\rho\mu)_r u_e\}. \quad (32)$$

The boundary conditions at the outer edge of the boundary layer are as follows,

$$f'(\xi, \eta_\delta) = 1 \quad (33)$$

$$\theta(\xi, \eta_\delta) = 1 \quad (34)$$

$$\zeta_i(\xi, \eta_\delta) = \zeta_{ie} \qquad i = 1\text{–}5. \quad (35)\text{–}(39)$$

The values of ζ_{ie} in equations (35)–(39) are decided from the condition of the free stream flow.

The boundary conditions at the leading edge are determined by substituting $\xi = 0$ into equations (16)–(22), that is,

$$\frac{dV}{d\eta} + f' = 0$$

or

$$V = -\int_0^\eta f'\,d\eta \equiv -f$$

$$-f\frac{df'}{d\eta} = \frac{d}{d\eta}\left(A\frac{df'}{d\eta}\right),$$

$$-f\frac{d\theta}{d\eta} = \frac{d}{d\eta}\left(B\frac{d\theta}{d\eta} + \sum_{i=1}^{5} C_i\frac{d\zeta_i}{d\eta}\right) + D$$

$$-f\frac{d\zeta_i}{d\eta} = \frac{d}{d\eta}\left(E_i\frac{d\zeta_i}{d\eta}\right)$$

$$i = 1\text{–}4.$$

As these ordinary differential equations can be easily solved, the boundary conditions at the leading edge are given as follows by taking account of equation (23).

$$f(0, \eta) = f'_0(\eta) \quad (40)$$

$$V(0, \eta) = V_0(\eta) \quad (41)$$

$$\theta(0, \eta) = \theta_0(\eta) \quad (42)$$

$$\zeta_i(0, \eta) = \zeta_{i_0}(\eta) \qquad i = 1\text{–}5. \quad (43)\text{–}(47)$$

The profiles of temperature and concentrations of species determined by solving the above governing equations on the above boundary conditions are refered to the dimensionless quantities θ and ζ_1–ζ_5. In order to get the profiles of quantities t and W_1–W_5 from the above results, it is necessary to evaluate t_w and W_{1w}–W_{5w} from the following boundary conditions.

From the energy balance at the wall, the following equation is obtained.

$$-\frac{1}{Pr}\left\{\Delta h\frac{\partial\theta}{\partial\eta} - \sum_{i=1}^{5} h_{i_w}\frac{\partial W_i}{\partial\eta}\right\}_{\eta=0} = V(\xi, 0)\,(L + h_w - h_t). \quad (48)$$

The flow passing across the upper surface of the test plate consists of fuel vapor only, for which we get the following relation

$$V(\xi, 0) = \left\{\frac{-\rho D_1 W_{1r}}{\mu(1 - W_1)}\frac{\partial\zeta_1}{\partial\eta}\right\}_{\eta=0} \quad (49)$$

$$V(\xi, 0) = \left\{\frac{\rho D_i W_{ir}}{\mu W_i}\frac{\partial\zeta_i}{\partial\eta}\right\}_{\eta=0} \qquad i = 2\text{–}5. \quad (50)\text{–}(53)$$

As the fuel vapor must be saturated at the wall, the mass fraction of fuel at the wall W_{1w} can be determined from the wall temperature t_w as follows.

$$W_{1w} = \varphi(t_w). \quad (54)$$

Substituting a suitable first order approximate value of t_w into equation (54), we can have W_{1w}. And again by substituting W_{1w} into equation (49), $V(\xi, 0)$ is determined. The second order approximate value of t_w can be computed by

substituting the above result of $V(\xi, 0)$ into equation (48).

By repeating the above procedure, the accurate values of t_w and W_{1w} could be determined. The mass fractions of species at the wall except fuel vapor W_{2w}–W_{5w} can be calculated by substituting $V(\xi, 0)$ into equations (50)–(53). The mass flow passing across the upper surface of the test plate $(\rho v)_w$ can be calculated from equation (32).

In the case with impermeable leading section, taking ξ^*–η^* coordinates from the leading edge of the impermeable section, we can have the velocity profile by solving equations (16) and (17) for these coordinates. As the next step, the velocity profile is transformed into ξ–η coordinates which are taken from the leading edge of the permeable section. By substituting this transformed velocity profile into equations (18)–(23), the profiles of temperature and concentrations of species for this case with the impermeable leading section can be calculated.

3. NUMERICAL CALCULATION AND PROPERTIES

As it may be very difficult to solve the above governing equations by analytical method, in present paper, the finite difference method was used to get the numerical solution of this problem.

Equations (17)–(23) are represented with the implicit scheme as follows respectively.

Equation of momentum,

$$\alpha_{fm+1,n} f'_{m+1,n+1} + \beta_{fm+1,n} f'_{m+1,n} + \gamma_{fm+1,n} f'_{m+1,n-1} = \delta_{fm+1,n} \tag{55}$$

$$\alpha_{fm+1,n} = (V_{m+1,n}/2\Delta\eta) - \{(A_{m+1,n+1} - A_{m+1,n-1})/4\Delta\eta^2\} - (A_{m+1,n}/\Delta\eta^2)$$

$$\beta_{fm+1,n} = 2\{(\xi_{m+1} f'_{m+1,n}/\Delta\xi) + (A_{m+1,n}/\Delta\eta^2)\}$$

$$\gamma_{fm+1,n} = -(V_{m+1,n}/2\Delta\eta) + \{(A_{m+1,n+1} - A_{m+1,n-1})/4\Delta\eta^2\} - (A_{m+1,n}/\Delta\eta^2)$$

$$\delta_{fm+1,n} = 2\xi_{m+1} f'_{m+1,n} f'_{m,n}/\Delta\xi$$

Equation of energy,

$$\alpha_{\theta m+1,n}\theta_{m+1,n+1} + \beta_{\theta m+1,n}\theta_{m+1,n} + \gamma_{\theta m+1,n}\theta_{m+1,n-1} = \delta_{\theta m+1,n} \tag{56}$$

$$\alpha_{\theta m+1,n} = (V_{m+1,n}/2\Delta\eta) - \{(B_{m+1,n+1} - B_{m+1,n-1})/4\Delta\eta^2\} - (B_{m+1,n}/\Delta\eta^2)$$

$$\beta_{\theta m+1,n} = 2\{(\xi_{m+1} f'_{m+1,n}/\Delta\xi) + (B_{m+1,n}/\Delta\eta^2)\}$$

$$\gamma_{\theta m+1,n} = -(V_{m+1,n}/2\Delta\eta) + \{(B_{m+1,n-1} - B_{m+1,n-1})/4\Delta\eta^2\} - (B_{m+1,n}/\Delta\eta^2)$$

$$\delta_{\theta m+1,n} = (2\xi_{m+1} f'_{m+1,n}\theta_{m,n}/\Delta\xi) + \{\sum_{i=1}^{5} (C_{im+1,n+1} - C_{im+1,n-1}) \times (\zeta_{im+1,n+1} - \zeta_{im+1,n-1})/4\Delta\eta^2\} + \{\sum_{i=1}^{5} C_{im+1,n}(\zeta_{im+1,n+1} - 2\zeta_{im+1,n} + \zeta_{im+1,n-1})/\Delta\eta^2\} + D_{m+1,n}$$

Equation of continuity of species,

$$\alpha_{im+1,n}\zeta_{im+1,n+1} + \beta_{im+1,n}\zeta_{im+1,n} + \gamma_{im+1,n}\zeta_{im+1,n-1} = \delta_{im+1,n} \qquad i = 1\text{–}4 \tag{57)–(60}$$

$$\alpha_{im+1,n} = (V_{m+1,n}/2\Delta\eta) - \{(E_{im+1,n+1} - E_{im+1,n-1})/4\Delta\eta^2\} - (E_{im+1,n}/\Delta\eta^2)$$

$$\beta_{im+1,n} = 2\{(\xi_{m+1} f'_{m+1,n}/\Delta\xi) + (E_{im+1,n}/\Delta\eta^2)\}$$

$$\gamma_{im+1,n} = -(V_{m+1,n}/2\Delta\eta) + \{(E_{im+1,n+1} - E_{im+1,n-1})/4\Delta\eta^2\} - (E_{im+1,n}/\Delta\eta^2)$$

$$\delta_{im+1,n} = (2\xi_{m+1} f'_{m+1,n}\zeta_{im,n}/\Delta\xi) + F_{im+1,n}$$

$$\sum_{i=1}^{5} \zeta_{im,n} W_{ir} = 0 \tag{61}$$

where, subscripts m and n denote the value at the station $\xi = m\Delta\xi$, and $\eta = n\Delta\eta$ as shown in Fig. 2.

$X_{m+1}(X: A, B, C_i, \zeta_i$ and $E_i)$ in equations (55)–(61) are unknown quantities, therefore the successive approximation method must be used

to solve these equations by assuming $X_{m+1} \cong X_m$ as the first order approximation. As the first step, let us consider to solve the equation of momentum equation (55) on the boundary conditions equations (25) and (33).

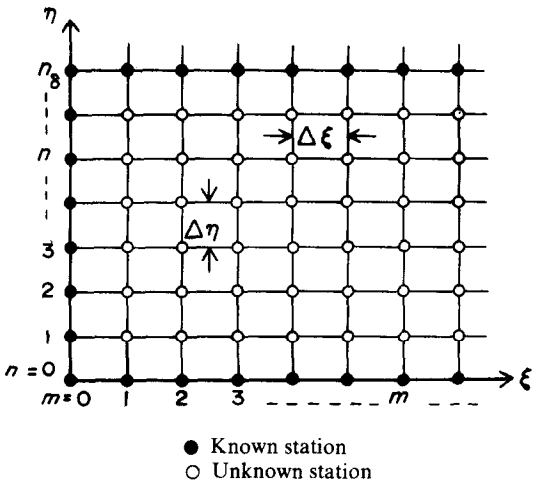

FIG. 2. Finite difference grid.

It is impossible to solve equation (55) because it has three unknown quantities $f'_{m+1,n+1}$, $f'_{m+1,n}$ and $f'_{m+1,n-1}$. However, dividing the domain from the wall to the outer edge of the boundary layer into n_δ sections as shown in Fig. 2, $(n_\delta - 1)$ unknown quantities i.e. $f'_{m+1,1} \sim f'_{m+1,n\delta-1}$ are contained in this domain, and $(n_\delta - 1)$ equations which have three unknown quantities as mentioned above, are available. Therefore, the velocity profile could be decided by solving these $(n_\delta - 1)$ equations simultaneously.

Even in the case of laminar boundary layer discussed in present paper, it is recommended to take $n_\delta \cong 80$. This fact shows that it might be terribly laborious to solve these equations simultaneously. In this paper, the procedure proposed by F. G. Blottner [11] was used to solve these equations as follows.

Let us assume the solution in the following form

$$f'_{m+1,n} = G_{m+1,n} f'_{m+1,n+1} + H_{m+1,n}. \tag{62}$$

This equation implies that

$$f'_{m+1,n-1} = G_{m+1,n-1} f'_{m+1,n} + H_{m+1,n-1}. \tag{63}$$

Substituting equation (63) into equation (55) and comparing with equation (62), we get the following results.

$$G_{m+1,n} = -\frac{\alpha_{fm+1,n}}{\beta_{fm+1,n} + \gamma_{fm+1,n} G_{m+1,n-1}} \tag{64}$$

$$H_{m+1,n} = \frac{\delta_{fm+1,n} - \gamma_{fm+1,n} H_{m+1,n-1}}{\beta_{fm+1,n} + \gamma_{fm+1,n} G_{m+1,n-1}}.$$

As $f'_{m+1,0} = 0$ at the wall $(n = 0)$ and $f'_{m+1,1} \neq 0$ at $n = 1$, we get

$$G_{m+1,0} = 0, \qquad H_{m+1,0} = 0. \tag{65}$$

Substituting the above results into equation (64), we can get $G_{m+1,1}$ and $H_{m+1,1}$. By repeating this procedure, all G_{m+1}'s and H_{m+1}'s up to $G_{m+1,n\delta-1}$ and $H_{m+1,n\delta-1}$ across the boundary layer are determined, and then f'_{m+1}'s can be found from equation (62).

In order to calculate the values of $G_{m+1,n}$ and $H_{m+1,n}$ in equation (64), the value of $V_{m,n}$ contained in $\alpha_{fm,n}$ and $\gamma_{fm,n}$ must be found. From equation (16), the following finite difference equation is obtained.

$$\begin{aligned} V_{m+1,n+1} = {} & V_{m+1,n} - V_{m,n+1} + V_{m,n} \\ & - \{2\xi_{m+\frac{1}{2}}(f'_{m+1,n+1} - f'_{m,n+1} \\ & + f'_{m+1,n} - f'_{m,n})/\Delta\xi + (f'_{m+1,n+1} \\ & + f'_{m+1,n} + f'_{m,n+1} + f'_{m,n})/2\}\,\Delta\eta. \end{aligned} \tag{66}$$

Since the values of $V_{0,n}$ and $V_{m,0}$ are known quantities from the boundary conditions equations (41) and (49), the value of V at every station can be decided from equation (66) in order of $V_{1,1} \to V_{1,n}$, $V_{2,1} \to V_{2,n}$, $\cdots$ $V_{m,1} \to V_{m,n}$.

The profiles of temperature and concentrations of species across the boundary layer can be determined by the same procedure.

The properties of mixed gas were calculated by the following equations.

The specific heat at constant pressure of the mixed gas is

$$c_p = \sum_{i=1}^{5} W_i c_{pi}. \tag{67}$$

The coefficient of dynamic viscosity of the mixed gas is [12]

$$\mu = \sum_{i=1}^{5} \frac{(W_i/M_i)\,\mu_i}{\sum_{j=1}^{5} (W_j/M_j)\phi_{ij}},$$

$$\phi_{ij} = \frac{1}{\sqrt{(8)}}\left(1 + \frac{M_i}{M_j}\right)\left\{1 + \left(\frac{\mu_i}{\mu_j}\right)^{\frac{1}{2}}\left(\frac{M_j}{M_i}\right)\right\}^2. \tag{68}$$

The thermal conductivity of the mixed gas is [13]

$$\lambda = \sum_{i=1}^{5} \frac{(W_i/M_i)\,\lambda_i}{\sum_{j=1}^{5} (W_j/M_j)\,\phi_{ij}}. \tag{69}$$

The multicomponent diffusion coefficient of species i is [14]

$$D_i = \frac{N_i - x_i \sum_{j=1}^{5} N_j}{c\{\sum_{j=1}^{5} (1/c\,\mathscr{D}_{ij})(x_j N_i - x_i N_j)\}} \tag{70}$$

$$c = \sum_{i=1}^{5} c_i, \qquad c_i = \rho g W_i/M_i, \qquad x_i = c_i/c.$$

$$N_i = -cD_i(\mathrm{d}x_i/\mathrm{d}y).$$

The properties of each species are given in [15] and [16] as the functions of temperature and pressure.

4. CALCULATED RESULTS AND CONSIDERATIONS

According to the above procedure, calculations were carried out on the conditions tabulated in Table 1. The parentheses in Table 1 show the cited reference. $u_e = 1$ m/s and $t_e = 20°C$ were chosen as the velocity and temperature of the free stream flow. The saturated pressures

Table 1. Conditions of calculation

No.	Fuel	x (mm)	v_w (mm/s)	l (mm)	E_A (kcal/mol)	L (kcal/kg)	Q (kcal/kg)	Atmosphere	Property
1	CH_3OH	0	—	0	0	263	4800	Air	Air
2	CH_3OH	0	—	0	0	263	4800	Air	Mixed gas
3	CH_3OH	105	—	0	41·3 [17]	263	4800	Air	Mixed gas
4	C_2H_5OH	105	—	0	42·2 [17]	206	6400	Air	Mixed gas
5	C_2H_5OH	105	—	0	0	206	6400	Air	Mixed gas
6	CH_3OH	105	—	0	41·3	263	4800	Air	Mixed gas
7	CH_3OH	105	—	0	0	263	4800	Oxygen	Mixed gas
8	CH_3OH	15	—	25	41·3	263	4800	Oxygen	Mixed gas
9	CH_3OH	55	—	25	41·3	263	4800	Air	Mixed gas
10	C_3H_8	30	3	0	0	—	12033	Air	Mixed gas
11	C_3H_8	75	3	0	0	—	12033	Air	Mixed gas
12	C_3H_8	105	3	0	0	—	12033	Air	Mixed gas
13	C_3H_8	30	3	0	26·0 [18]	—	12033	Air	Mixed gas
14	C_3H_8	75	3	0	26·0	—	12033	Air	Mixed gas
15	C_3H_8	105	3	0	26·0	—	12033	Air	Mixed gas

for methyl alcohol and ethyl alcohol are represented by the following formulae [19]

$$W_{1w} = (M_1/M)\exp\{(t_w - 64{\cdot}7)/22{\cdot}8\}$$

methyl alcohol

$$W_{1w} = (M_1/M)\exp\{(t_w - 77{\cdot}8)/23{\cdot}2\}$$

ethyl alcohol.

Figure 3 corresponds to the condition 1 in Table 1. It is well known that the boundary layer approximation is not available near the leading edge, but according to the calculated

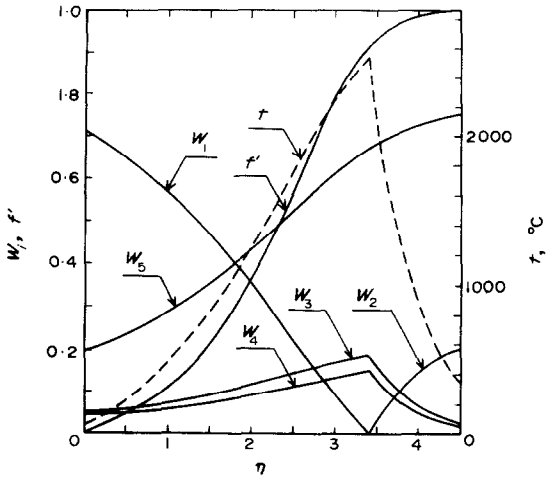

FIG. 3. Profiles of velocity, temperature and concentrations of species (properties are function of temperature only).

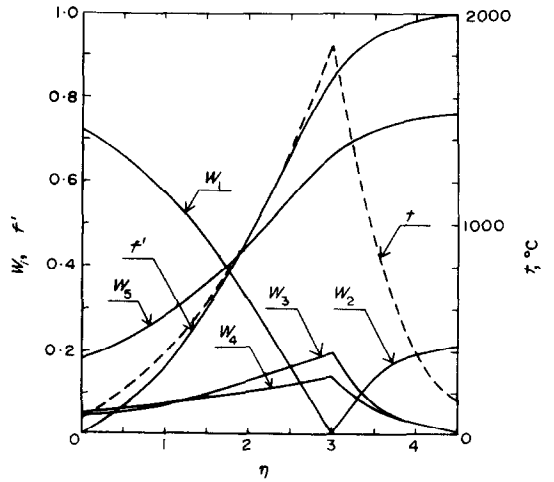

FIG. 4. Profiles of velocity, temperature and concentrations of species (properties are function of temperature and concentrations of species).

results, the profiles represented in η coordinate were almost independent of the distance from the leading edge. Figure 3 shows that the flame sheet is kept at $\eta \cong 3{\cdot}4$ and the maximum temperature at the flame sheet is about 2500°C.

The results on 2nd condition in Table 1 are depicted in Fig. 4. Comparing Fig. 4 with Fig. 3 it can be seen that by taking account of the effect of concentration on properties, the maximum temperature goes down about 700°C, the location of flame sheet shifts to the wall, and the profiles of concentrations of water vapor and carbon dioxide cross each other at $\eta \cong 1{\cdot}2$.

Most of the papers on combustion process which have been published until now assume that the properties are constant or functions of temperature only. It must be noted, however, that these assumptions about properties are very contradictory to the fact, therefore, the quantitative comparison of the calculated result with the experimental one would be meaningless.

The calculated results on the condition 3 in Table 1 are shown in Fig. 5, and the same results are represented with respect to the physical coordinate y in Fig. 6. All profiles in these figures are markedly different from those in Fig. 4. First of all, the flame sheet vanishes from

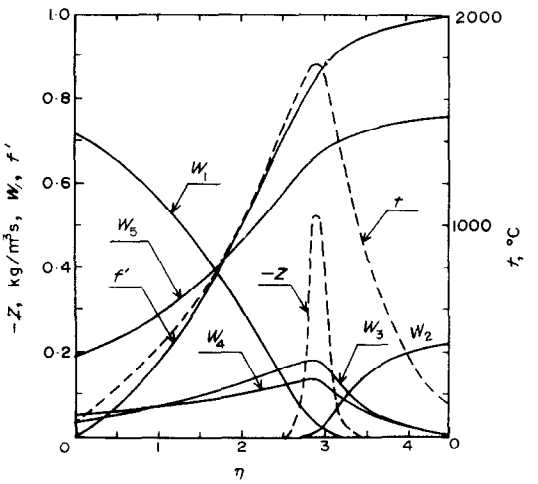

FIG. 5. Profiles of velocity, temperature, mass rate of combustion and concentrations of species (finite rate of chemical reaction).

Figs. 5 and 6, and these profiles show the combustion zone having the finite width. The profiles of temperature and concentrations of

carbon dioxide and water vapor in Fig. 4 have the sharp summits at the flame sheet, and those in Fig. 5 are round, consequently, the maximum values of temperature and concentrations of these species diminish. The maximum temperature in Fig. 5 is about 80°C lower than that in Fig. 4. The position where the temperature becomes summit shifts a little to the wall by introducing the Arrhenius' theory.

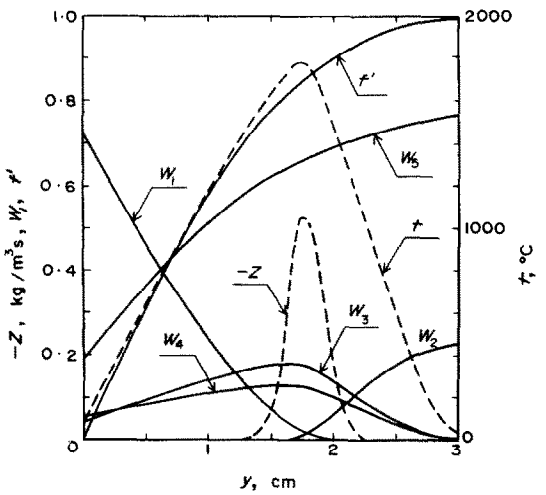

FIG. 6. Profiles of velocity, temperature, mass rate of combustion and concentrations of species (in physical coordinate).

Taking y coordinate as the abscissa, the layers adjacent to the wall and to the outer edge of the boundary layer shrink and the combustion zone is expanded as easily seen from equation (15). Consequently, as is shown in Fig. 6, most of the inflection points vanish from the curves. It was made sure that the velocity profile in Fig. 6 is almost the same as the Blasius' velocity profile for laminar boundary layer without mass injection.

Figure 7 shows the profiles of Lewis numbers of species, Prandtl number and density. As is seen from Fig. 6, the temperature varies from 20°C to about 1800°C in the boundary layer, and with the change of temperature the coefficients of dynamic viscosity of species vary 3–5 times, the thermal conductivities 4–12 times and the multicomponent diffusion coefficients 20–25 times, respectively. However, the changes of Lewis number and Prandtl number assembled with these properties are much less than that of

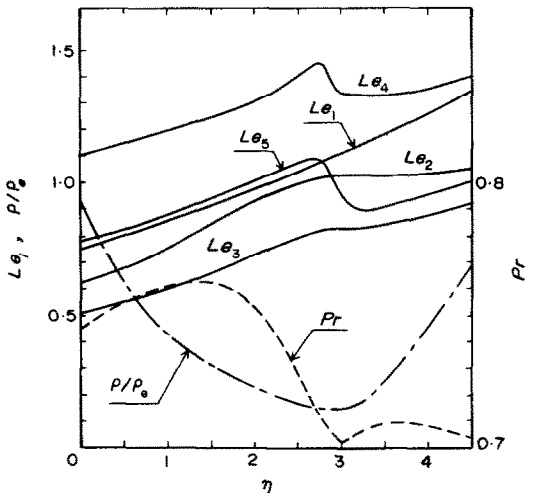

FIG. 7. Profiles of properties.

individual property. Most investigations on combustion process have assumed that Prandtl number and Lewis number are unity across the boundary layer, but the complex behaviors of them near the combustion zone in Fig. 7 imply the lack of validity of this assumption.

In this paper, the upper and lower boundaries of combustion zone y_{out} and y_{in} are defined as shown in Fig. 8. The upper and lower boundaries of combustion zone, the outer edges of hydrodynamic, thermal and concentration boundary layers, the heat flux at the wall and the mass transfer ratio are represented in Fig. 9. The outer edges of the hydrodynamic and concentration boundary layers are defined as the points at which the value of velocity or concentration becomes 99 per cent of that in free stream flow. The outer edge of the thermal boundary layer is the point at which $(t - t_e)/(t_{max} - t_e) = 0{\cdot}01$.

The mass transfer ratio is defined as follows; $\beta = (\rho v)_w/(\rho u)_e$. The combustion zone occupies

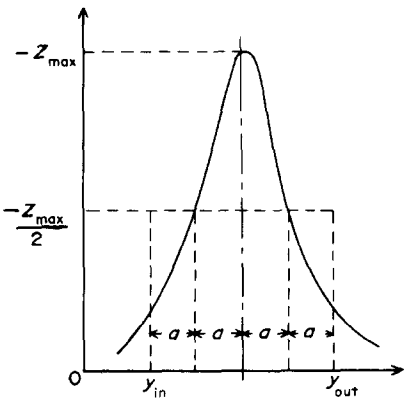

FIG. 8. Definition of combustion zone.

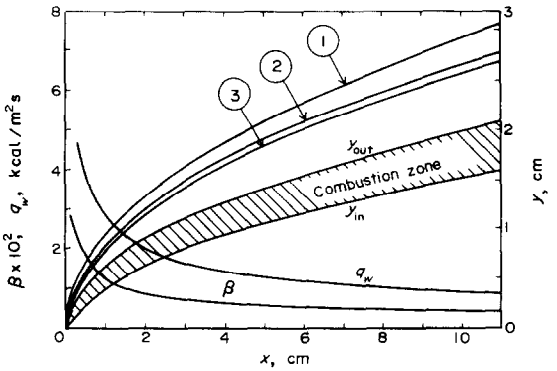

FIG. 9. Outer edges of boundary layers, combustion zone, heat flux and mass transfer ratio.

① Outer edge of thermal boundary layer.
② Outer edge of concentration boundary layer.
③ Outer edge of hydrodynamic boundary layer.

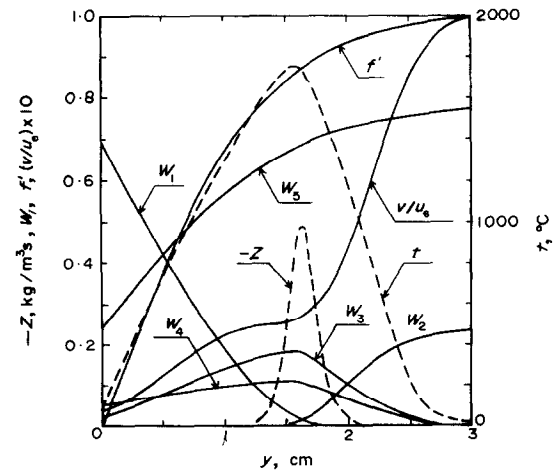

FIG. 10. Profiles of velocities, temperature, mass rate of combustion and concentrations of species (ethyl alcohol).

about 20 per cent of the boundary layer in width.

Figure 10 shows the results for ethyl alcohol (Condition 4 in Table 1). The calorific value of ethyl alcohol is higher than that of methyl alcohol, on the other hand, the specific heat of ethyl alcohol is larger than that of methyl alcohol. In consequence of the above two opposite factors, it seems that the temperature profile of ethyl alcohol in Fig. 10 is very similar to that of methyl alcohol.

The following equation can be reduced from equation (24).

$$v = \frac{(\rho\mu)_r u_e}{\sqrt{(2\xi)}\rho}(V + f'\eta) - f'\frac{\sqrt{(2\xi)}}{\rho}\int_0^\eta \frac{1}{\rho}\frac{\partial\rho}{\partial x}\,d\eta.$$

An example of the profile of velocity v calculated from the above equation is represented in Fig. 10.

The close up of the combustion zone in Fig. 10 is shown with dotted lines in Fig. 11. For

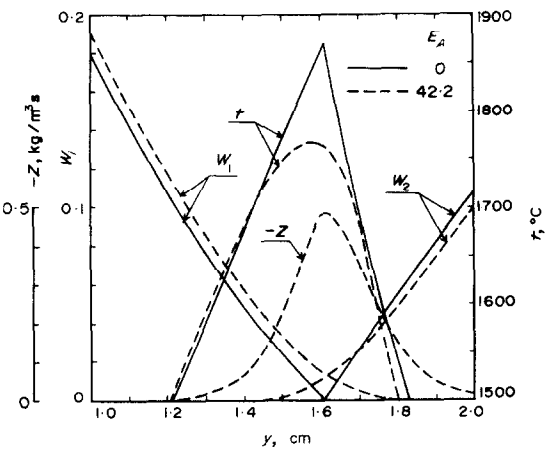

FIG. 11. Detail in combustion zone and its vicinity (comparison with flame sheet model).

comparison, the result for the flame sheet model (Condition 5 in Table 1) is shown with solid lines in the same figure. The maximum temperature for the flame sheet model is about 100°C higher than that for the finite rate of

chemical reaction. The general tendency is similar to the result for methyl alcohol.

The combustion process in the oxygen stream flow was calculated for the cases of finite and infinite rates of chemical reaction (Conditions 6 and 7 in Table 1). These results are represented in Fig. 12. The difference of maximum temperatures for both cases is about 200°C, and this temperature difference is two times larger than that in the air stream.

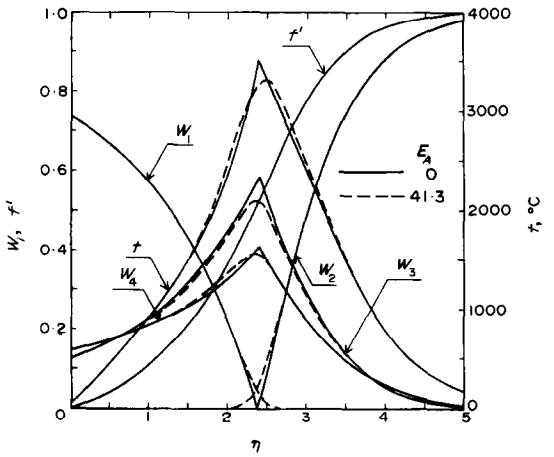

FIG. 12. Profiles of velocity, temperature and concentrations of species (combustion in oxygen).

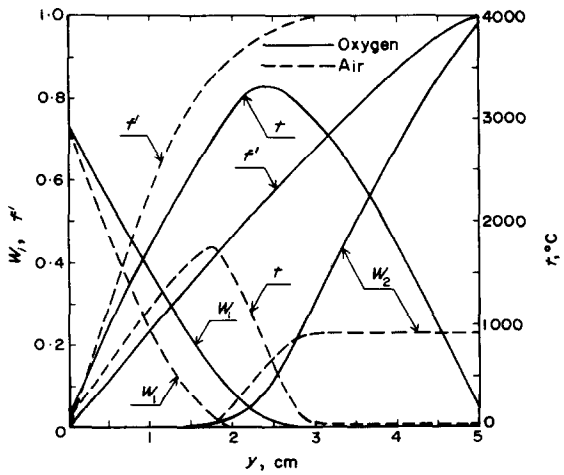

FIG. 13. Profiles of velocity, temperature and concentrations of species (comparison of air with oxygen).

The comparison of the results for air stream and oxygen stream is shown in Fig. 13. The maximum temperature and the boundary layer thickness in the oxygen stream becomes about twice those in the air stream and the velocity profile approaches a straight line.

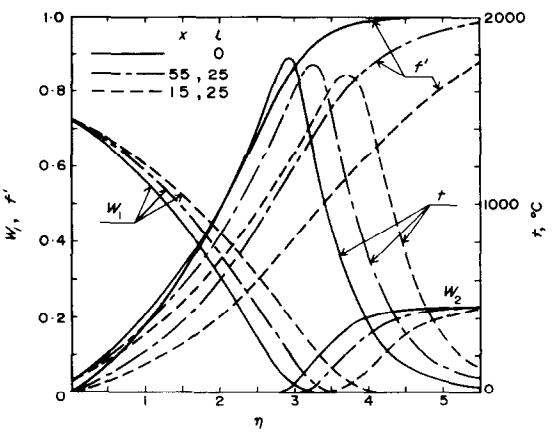

FIG. 14. Profiles of velocity, temperature and concentrations of species (effect of impermeable leading section).

In the all aforementioned results, every profile represented with respect to η was nearly independent of ξ. In the matter of fact, the cases without impermeable leading section are rather few, therefore it is important to clarify the effect of impermeable leading section on the combustion process in the boundary layer. The effect of impermeable leading section will be discussed in the following. The results with impermeable leading section of 2·5 cm long are represented in Fig. 14 (Conditions 8 and 9 in Table 1). To make clear the effect of the impermeable leading section, the results without impermeable leading section are shown in the same figure (Condition 3 in Table 1).

As already mentioned, the profiles of velocity, temperature and concentrations of species for the case without impermeable leading section are almost independent of the distance from the leading edge, if the dimensionless coordinate η is taken as an abscissa. However, in the case

with impermeable leading section, the profiles depend on the distance from the leading edge. It is seen that the boundary layer gets thicker and the maximum temperature lower with impermeable leading section. However, the effect of impermeable leading section decreases with increasing the distance from leading edge of permeable section x. To study the effect of the impermeable leading section more precisely, the calculations at many stations of x were carried out, and the results are shown in Fig. 15. The length of 2·5 cm was adopted as the impermeable leading section l in these calculations.

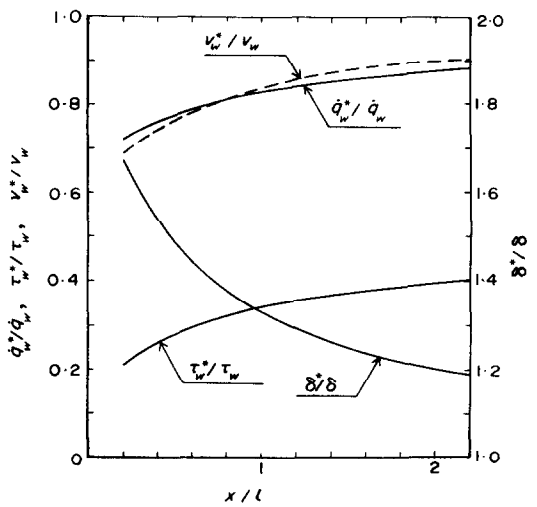

FIG. 15. Effect of impermeable leading section on vaporization rate, heat flux, shear stress and boundary layer thickness.

The heat flux, the injection velocity and shear stress at the wall in the case with impermeable leading section are lower than those in the case without impermeable leading section, but the differences between them decrease with x. The effect of the impermeable leading section on the shear stress at the wall is most remarkable.

In the foregoing, we have discussed the combustion process of the liquid fuels, and then we shall discuss the gaseous fuel uniformly injected from the permeable plate. Figure 16 represents the combustion process of propane for the flame sheet model (Conditions 10, 11 and 12 in Table 1) and Fig. 17 shows for the

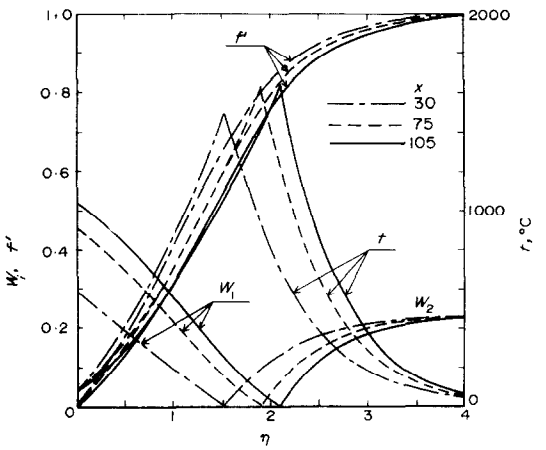

FIG. 16. Profiles of velocity, temperature and concentrations of species (uniform injection of propane).

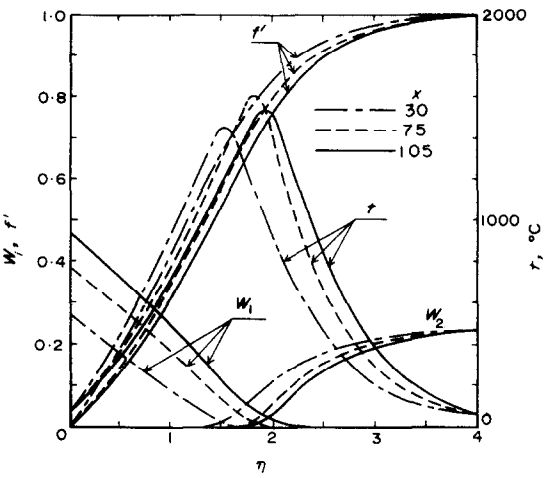

FIG. 17. Profiles of velocity, temperature and concentrations of species (finite rate of chemical reaction).

case of finite rate of chemical reaction (Conditions 13, 14 and 15 in Table 1). In these figures the fuel concentration at the wall, the profiles of velocity, temperature and concentrations of species and the maximum temperature vary with

the distance from the leading edge. The maximum temperature near the leading edge is lower than that at downstream in these figures. This tendency might be owing to that the heat flux near the leading edge is relatively larger than that at downstream, on the other hand the injection rate of the fuel is uniform throughout the wall.

5. CONCLUSIONS

As the result of the theoretical investigation on the combustion process of liquid and gaseous fuels in the laminar boundary layer on a flat plate, the following conclusions have been obtained.

(1) By taking into account that the properties of fluid in the boundary layer depend on the temperature and the concentrations of species, the maximum temperature decreases by about several hundred degrees of centigrade.

(2) By introducing the Arrhenius' theory of chemical kinetics, the profiles of temperature and concentrations of species in the boundary layer considerably change and the maximum temperature diminishes by about 100°C.

(3) The coefficient of dynamic viscosity, the thermal conductivity and the multicomponent diffusion coefficient in the boundary layer vary in the very wide range, but the changes of Lewis number and Prandtl number are not remarkable.

(4) The combustion zone occupies about 20 per cent of the boundary layer in width.

(5) In the case without impermeable leading section, the profiles of velocity, temperature and concentrations of species with respect to the dimensionless coordinate η are almost independent of the distance from the leading edge.

(6) In the case with impermeable leading section, the boundary layer thickness increases and the maximum temperature goes down. The impermeable leading section have a great influence on the shear stress at the wall.

(7) Uniformly injecting the gaseous fuel from the wall, the fuel concentration at the wall and the maximum temperature change with the distance from the leading edge x. The profiles of velocity, temperature and concentrations of species with respect to η change in direction of x.

ACKNOWLEDGEMENTS

The authors wish to thank Professor W. H. Giedt and Professor H. A. Dwyer for many helpful suggestions.

REFERENCES

1. G. A. E. Godsave, Studies of the combustion of drops in a fuel spray–the burning of single drops of fuel. *4th Symposium (International) on Combustion*, pp. 818–830 (1953).
2. T. Okazaki and M. Gomi, The combustion and evaporation of a fuel droplet, *Trans. J.S.M.E.* **19**, 1–6 (1953).
3. M. Goldsmith and S. S. Penner, On the burning of single drops of fuel in an oxidizing atmosphere, *Jet Propulsion* **24**, 245–251 (1954).
4. H. Wise, J. Lorell and B. J. Wood, The effect of chemical and physical parameters on the burning rate of a liquid droplet, *5th Symposium (International) on Combustion*, pp. 132–141 (1955).
5. H. W. Emmons, The film combustion of liquid fuel, *Z. Angew. Math. Mech.* **36**, 60–71 (1956).
6. A. Q. Eschenroder, Combustion in the boundary layer on a porous surface, *J. Aerospace Sci.* 901–906 (1960).
7. Y. Nakagawa, N. Nishiwaki and M. Hirata, Effect of combustion on a laminar boundary layer, *13th Symposium (International) on Combustion*, pp. 813–819 (1971).
8. J. Lorell, H. Wise and R. E. Carr, Steady-state burning of a liquid droplet, II. Bipropellant flame, *J. Chem. Phys.* **25**. 325–331 (1956).
9. F. E. Fendell, Ignition and extinction in combustion of initially unmixed reactants, *J. Fluid Mech.* **21**, Part 2, 281–303 (1965).
10. Y. Mori, K. Ohtaka, D. Nase and T. Tanozaki, Thermodynamic and electrical properties of combustion gas and its plasma, *Bull. J.S.M.E.* **12**, 883–893 (1969).
11. F. G. Blottner, Finite difference methods of solution of the boundary layer equation, *AIAA Jl* **8**, 193–205 (1970).
12. R. B. Bird, W. E. Stewart and E. N. Lightfoot, *Transport Phenomena*, p. 24. John Wiley, New York (1960).
13. R. B. Bird, W. E. Stewart and E. N. Lightfoot, *Transport Phenomena*, p. 258. John Wiley, New York (1960).
14. R. B. Bird, W. E. Stewart and E. N. Lightfoot, *Transport Phenomena*, p. 571. John Wiley, New York (1960).
15. H. Tong, *Simplified Analytic Functions for the Calculation of Thermodynamic and Transport Properties*, The Boeing Company Document D-2 1132B-1.

16. The Society of Chemical Engineers, Japan, *The Tables of Properties*, Vol. 8, p. 229. Maruzen, Tokyo (1971).
17. S. S. PENNER and B. P. MULLINS, *Explosions, Detonations, Flammability and Ignition*, p. 229. Pergamon Press, New York (1959).
18. J. B. FENN and H. F. CALCOTE, Activation energies in high temperature combustion, *4th Symposium (International) on Combustion*, pp. 231–239 (1953).
19. The Society of Chemical Engineers, Japan, *Handbook of Chemical Engineering*, p. 23. Maruzen, Tokyo (1961).

RECHERCHE THEORIQUE SUR LA COUCHE LIMITE LAMINAIRE AVEC COMBUSTION SUR UNE PLAQUE PLANE

Résumé—Les problèmes de la couche limite laminaire où se produit la réaction de combustion sont résolus théoriquement en tenant compte de la théorie d'Arrhénius sur la cinétique chimique, de l'effet de la section d'attaque imperméable et du fait que les propriétés du fluide dépendent de la température et des concentrations des espèces contenues dans la couche limite. Des résultats de cette recherche on a tiré les conclusions suivantes:

(1) la température maximale obtenue dans cette étude est plus basse d'environ plusieurs centaines de degrés centigrades que celle obtenue par la méthode qui a été employée dans les articles publiés antérieurement.

(2) la zone de combustion occupe environ 20% de la couche limite en largeur.

(3) dans le cas d'utilisation d'une plaque d'essai avec une section d'attaque imperméable, l'épaisseur de la couche limite croît et la température maximale diminue comparée au cas utilisant la plaque d'essai sans section d'attaque imperméable. La section d'attaque imperméable a une grande influence sur la contrainte tangentielle à la paroi.

(4) dans le cas de l'injection uniforme de combustible gazeux depuis la paroi, la concentration de combustible à la paroi et la température maximale changent avec la distance au bord d'attaque.

THEORETISCHE UNTERSUCHUNG EINER LAMINAREN GRENZSCHICHT MIT VERBRENNUNG AN DER EBENEN PLATTE

Zusammenfassung—Die Probleme der laminaren Grenzschicht mit Verbrennungsreaktion wurden theoretisch gelöst mit dem Arrhenius-Ansatz für die chemische Kinetik, mit Berücksichtigung einer undurchdringlichen Anlaufstrecke und mit Berücksichtigung der Abhängigkeit der Stoffwerte von Temperatur und der chemischen Zusammensetzung der Grenzschicht. Als Ergebnis dieser Untersuchungen lassen sich folgende Schlüsse ziehen:

1. Die Maximaltemperatur liegt in der vorliegenden Arbeit mehr als 100 °C niedriger als bei den Methoden, die bei früher veröffentlichten Arbeiten verwendet wurden.
2. Die Verbrennungszone macht ungefähr 20% der Grenzschichtdicke aus.
3. Im Fall einer Platte mit undurchdringlicher Anlaufstrecke nimmt die Grenzschichtdicke zu und die Maximaltemperatur liegt niedriger, verglichen mit der Platte ohne undurchdringliche Anlaufstrecke. Die undurchdringliche Anlaufstrecke hat einen grossen Einfluss auf die Wandschubspannung.
4. Im Fall gleichmässiger Einblasung von Brennstoff durch die Wand verändert sich die Brennstoffkonzentration an der Wand und die Maximaltemperatur mit dem Abstand von der Anströmkante.

ТЕОРЕТИЧЕСКОЕ ИССЛЕДОВАНИЕ ЛАМИНАРНОГО ПОГРАНИЧНОГО СЛОЯ ПРИ ГОРЕНИИ НА ПЛОСКОЙ ПЛАСТИНЕ

Аннотация—Задача ламинарного пограничного слоя при наличии реакций горения решается теоретически на основании теории химической кинетики Аррениуса с учетом влияния непроницаемого начального участка, а также зависимости свойств жидкости от температуры и концентрации веществ, находящихся в пограничном слое. В результате этого исследования сделаны следующие выводы:

1. Максимальная темпаратура, полученная в данной работе, оказалась ниже температуры, полученной методами, используемыми в ранее опубликованных работах, примерно на несколько сот градусов.
2. Зона горения занимает по ширине примерно 20% пограничного слоя.
3. При использовании пластины с непроницаемым начальным участком толщина

пограничного слоя увеличивается, а максимальная температура снижается по сравнению с пластиной при отсутствии непроницаемого начального участка. Непроницаемый начальный участок оказывает большое влияние на напряжение трения на стенке.

4. В случае равномерного вдува газообразного топлива концентрация на стенке и максимальная температура изменяется по мере удаления от начального участка.